Plant Communications
Research article

CellPress
Partner Journal

Modeling the influence of phenotypic plasticity on maize hybrid performance

Ran Fu[1,2] and Xiangfeng Wang[1,2,*]

[1]National Maize Improvement Center, College of Agronomy and Biotechnology, China Agricultural University, Beijing 100094, China

[2]Frontiers Science Center for Molecular Design Breeding, College of Agronomy and Biotechnology, China Agricultural University, Beijing 100094, China

***Correspondence: Xiangfeng Wang (xwang@cau.edu.cn)**

https://doi.org/10.1016/j.xplc.2023.100548

ABSTRACT

Phenotypic plasticity, the ability of an individual to alter its phenotype in response to changes in the environment, has been proposed as a target for breeding crop varieties with high environmental fitness. Here, we used phenotypic and genotypic data from multiple maize (*Zea mays* L.) populations to mathematically model phenotypic plasticity in response to the environment (PPRE) in inbred and hybrid lines. PPRE can be simply described by a linear model in which the two main parameters, intercept *a* and slope *b*, reflect two classes of genes responsive to endogenous (class A) and exogenous (class B) signals that coordinate plant development. Together, class A and class B genes contribute to the phenotypic plasticity of an individual in response to the environment. We also made connections between phenotypic plasticity and hybrid performance or general combining ability (GCA) of yield using 30 F_1 hybrid populations generated by crossing the same maternal line with 30 paternal lines from different maize heterotic groups. We show that the parameters *a* and *b* from two given parental lines must be concordant to reach an ideal GCA of F_1 yield. We hypothesize that coordinated regulation of the two classes of genes in the F_1 hybrid genome is the basis for high GCA. Based on this theory, we built a series of predictive models to evaluate GCA *in silico* between parental lines of different heterotic groups.

Key words: phenotypic plasticity, genotype-by-environment interaction, genomic selection, hybrid performance, general combining ability

Fu R. and Wang X. (2023). Modeling the influence of phenotypic plasticity on maize hybrid performance. Plant Comm. **4**, 100548.

INTRODUCTION

Plants modify a variety of phenotypic traits in response to environmental conditions, from the metabolic and cellular levels to the plant architecture level. This phenotypic plasticity is enabled by a combination of genetic and environmental factors and their interactions (Bradshaw, 1965; Des Marais et al., 2013). Thus, the observed phenotype of an individual is usually expressed as $P = G + E + G\times E$, in which P is the phenotypic value that is affected by genotype G in environment E and by their interactions $G\times E$ (Baye et al., 2011). Dissecting the roles of environmental factors in shaping genetic and phenotypic plasticity is important for bolstering agricultural productivity under current climate change projections (Aspinwall et al., 2015). Temperature and day length are critical environmental factors that affect phenotypes in many crop species and are used in modeling of crop development (Robertson, 1968; Brachi et al., 2010; Blackman, 2017; Scheres and van der Putten, 2017). Therefore, identifying the effects of such environmental factors on crop yield would enhance our understanding of $G\times E$ interactions at genetic, genomic, and environmental levels (Malosetti et al., 2013; Des Marais et al., 2013).

Although the interplay between genes and the environment has been widely studied in multiple crop species using quantitative and population genetics approaches, the molecular mechanism underlying phenotypic plasticity remains largely elusive (Taylor et al., 2021). The genetic control of the final expressed phenotype, phenotypic plasticity, and trait developmental trajectory can be resolved by measuring the genetic effects of several loci in individual environments, reaction-norm parameters across environments, and growth curve parameters throughout the season (Mu et al., 2022). It is critical to consider plastic responses in applications such as crop breeding, because plants must respond to the environments to which they are subjected. Although variability in plasticity at the population

Published by the Plant Communications Shanghai Editorial Office in association with Cell Press, an imprint of Elsevier Inc., on behalf of CSPB and CEMPS, CAS.

level has received much attention, most studies have focused on inbred populations (Kusmec et al., 2017; Li et al., 2021). Fewer studies have examined the effect of phenotypic plasticity on hybrid performance or heterosis because of the complexity represented by hybrids with two sets of genomes from their biparental lines (Gage et al., 2017). Thus, exploring the patterns of biparental phenotypic plasticity in response to the environment may reveal aspects of hybrid performance that can aid hybrid breeding.

Phenotypic plasticity is crucial for crop productivity and is subjected to artificial selection in breeding because greater adaptive plasticity may maintain stable yield and quality in changing environments (Nicotra et al., 2010; Kusmec et al., 2018). From an ecological and evolutionary perspective, phenotypic plasticity may be a powerful means of adaptation (Kelly et al., 2012). Phenotypic plasticity and its relationship with agricultural performance were documented as early as about 1500 years ago in the ancient Chinese agricultural textbook *Qi Min Yao Shu*, written by the Chinese agronomist Jia Sixie in the Northern Wei Dynasty. One of the chapters describes the relationship between flowering time, plant height, and grain yield in crops as follows: "While the early-maturing crop features short plant height but high grain yield, the late-maturing crop features tall plant height but low grain yield."

Research on phenotypic plasticity targeting flowering time, plant height, and crop yield will thus help reveal the patterns and genetic basis of crop adaptation. A model or framework incorporating an environmental dimension is highly desirable for quantifying the genetic architecture of phenotypic plasticity (Wang et al., 2013). Phenotypic plasticity may respond to multiple variables in the environment. Chevin and Lande (2015) contend that the linear combination of environmental variables that serve as developmental cues for the plastic trait is the multivariate best linear predictor of changes in the optimum at evolutionary equilibrium (Chevin and Lande, 2015). Multiple environmental factors influence plant development, but their effects are too complex to be considered together in a single model. A meaningful dimensionality reduction approach is thus important for generating a unified index to summarize the essential factors that contribute most to phenotypic plasticity. The particular way in which a genotype varies in its expression across a range of environments can be described by genetically determined reaction norms (Larcher, 2003). Gratani (2014) argue that the reaction norm for any specific trait of a genotype can be visualized as a line or a curve on a two-dimensional plot of the environmental value versus the phenotypic value. Research by Li et al. (2018) on two simplified response norm parameters, intercept and slope, shows that they may aid in genome prediction and potentially reveal the genetic determinants that underlie the patterned differential responses of individuals to environmental conditions. The environmental dimension can be added to the genomic selection of complex traits using two reaction norm parameters, thus facilitating the establishment of optimally designed multi-environment trials for forecasting crop performance at regional or global scales (Li et al., 2021).

Hybrid maize breeding has enhanced grain production more than 8-fold since the 1930s (Duvick, 2001). The primary breeding goal is now to identify high-yielding hybrid commercial cultivars that can adapt well to the increasingly varied temperate growing conditions of maize. However, we know considerably less about how hybrid performance interacts with environmental changes and the associated phenotypic plasticity, which must be taken into account to improve the adaptation of future maize hybrids. The performance of hybrids is influenced by the expression of genes that control traits related to their stress tolerance and fitness (Chen, 2013). Hybrids contain novel genotypes obtained by biparental hybridization, and parental adaptive plasticity in response to the environment may affect hybrid performance. The combination of parental inbred lines is crucial for the formation of heterosis; it is usually described by the metrics general combining ability (GCA) and special combining ability, which indicates the breeding value of a parent (Rojas and Sprague, 1952). Breeding value prediction (GCA) is feasible given adequate data; however, predicting intra- and inter-motif interactions that contribute to special combining ability is a more difficult component of predicting hybrid performance. Whether and how the phenotypic plasticity of the biparental lines is related to their combining ability in the F_1 hybrids will be key to exploring adaptive plasticity. Answering these questions will help to identify superior parents that can be used in breeding programs or promising cross combinations for cultivar development. By comprehensively collecting environmental, multi-omics, and phenotypic data via big-data-driven platforms, we can predict hybrid performance in advance through the phenotypic plasticity of parental inbred lines, thereby improving the efficiency and stability of hybrid maize production.

In this study, we developed a linear model (phenotypic plasticity in response to the environment [PPRE]) using the phenotypic plasticity response to the environment, which adds an environmental dimension to genome-wide association studies (GWAS) and genomic selection (GS) of complex traits. Joint research on flowering time, plant height, and crop yield revealed the genetic basis of phenotypic plasticity. We analyzed the biological implications of the model parameters and the patterns of phenotypic plasticity displayed by the parental lines in response to the environment and demonstrated that the concordant response of biparental lines influences hybrid performance. This work provides a convenient and low-cost means for interrogating GCA without having to generate F_1 hybrids.

RESULTS

Phenotypic plasticity of maize inbred and hybrid lines

To model the phenotypic plasticity of maize inbred and hybrid lines in response to the environment, we used a set of previously published genotypic and phenotypic data from four maize populations (methods). The inbred population was composed of the complete-diallel design plus unbalanced breeding-like intercross (CUBIC) lines, consisting of 1404 lines used as the maternal pool to cross with paternal tester lines (Liu et al., 2020). One of the hybrid populations comprised 6210 F_1 hybrids generated by crossing 207 CUBIC lines with 30 paternal testers. The other two populations were F_1 hybrids generated by crossing the 1404 CUBIC lines as the female parents with two elite testers, Jing724 and Zheng58, which are widely used in

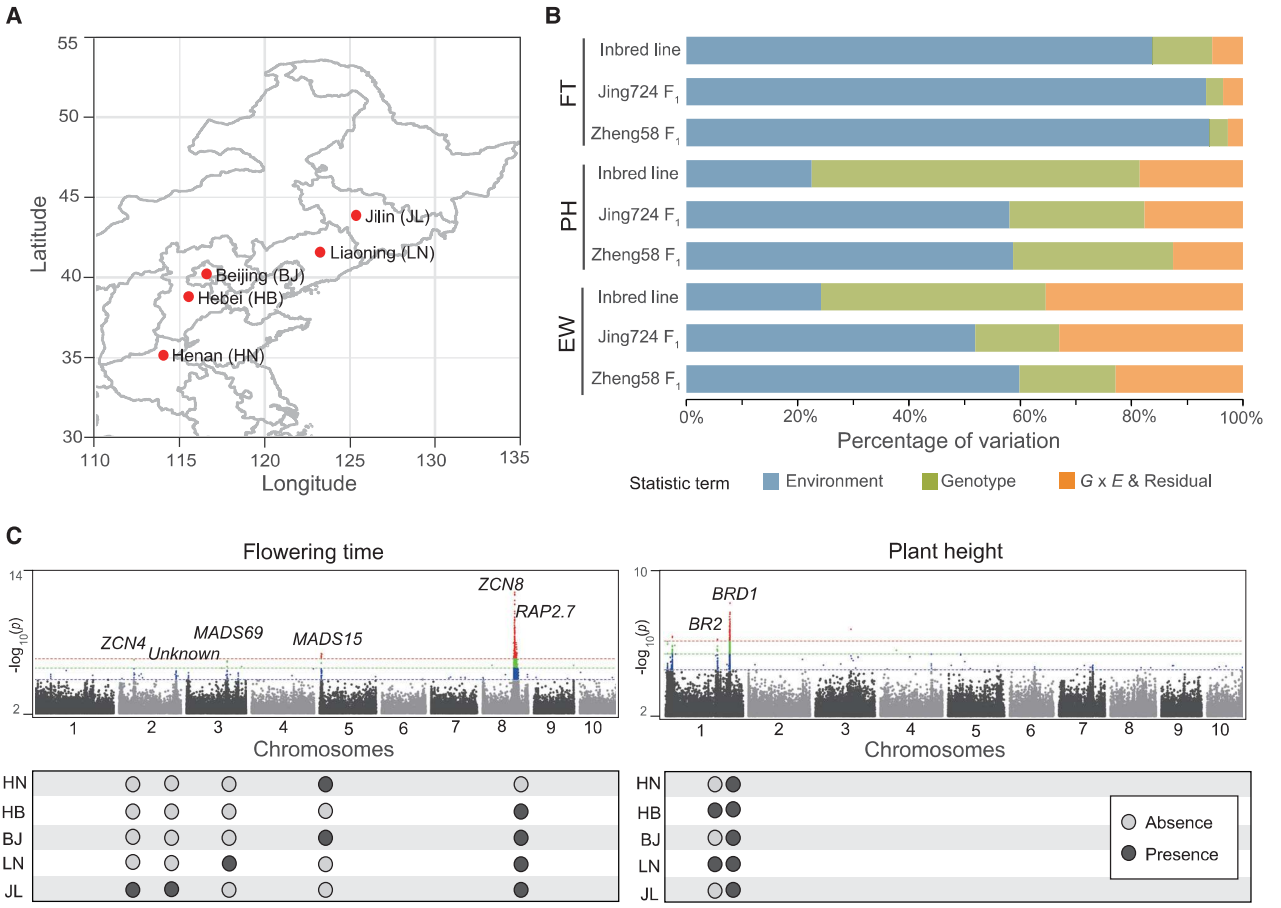

Figure 1. Phenotypic plasticity of maize inbred and hybrid lines.

(A) Geographic distribution of the five experimental locations.

(B) Summary of variance due to environment, genotype, or *G*×*E* with residual error for nine population–trait combinations. Three populations (1404 inbred population, Jing724 F_1 population, and Zheng58 F_1 population) and three traits (flowering time [FT], plant height [PH], and ear weight [EW]) were included.

(C) Manhattan plots from genome-wide association studies (GWASs) of the inbred population for FT (left) and PH (right) in five locations.

the maize breeding industry in China (Shu et al., 2021). All genotypes were phenotyped for three agronomic traits (flowering time [FT], plant height [PH], and ear weight [EW]) in five locations: Henan (35°31′N), Hebei (38°85′N), Beijing (40°13′N), Liaoning (41°48′N), and Jilin (43°88′N) (Figure 1A). As latitude increased across the five locations, FT for inbred and hybrid lines was gradually delayed, whereas PH and EW increased over the same latitudinal gradient, indicating the presence of phenotypic plasticity (Supplemental Figure 1).

We analyzed the individual contributions from the statistical terms genotype (*G*), environment (*E*), and *G*×*E* (with residual variance) to each phenotype and found different patterns for each of the three traits in inbred and hybrid lines (Figure 1B). For FT, *E* accounted for about 90% of the standing phenotypic variance in inbred and hybrid lines, indicating that the environment has a substantial influence on FT. For PH, *E* and *G* accounted for almost 20% and 60% of the phenotypic variance in inbred lines, respectively; however, the individual contributions of *E* and *G* for hybrid lines were approximately 60% and 20%. The contributions of *E* and *G* to PH variation were thus completely different in inbred and hybrid lines. This result indicated that the hybrid performance of PH is strongly influenced by the environment. We observed the same pattern for EW as for the first two traits, although the statistical term *G*×*E* made a greater contribution to EW phenotypic variation (35%), much greater than that seen for FT or PH. We therefore concluded that the hybrid performance of PH and EW is substantially influenced by *E* and *G*×*E*, which is likely attributable to the better performance of hybrid genomes in response to the environment compared with inbred genomes.

The heritability of the three traits of the maternal population is *H* (FT) = 0.87, *H* (PH) = 0.92, and *H* (EW) = 0.77, which is high enough to ensure the high quality of the phenotypic data collected at the five locations. We performed genetic mapping of FT and PH traits individually at each of the five locations to reveal the underlying mechanisms of phenotypic plasticity by focusing on specific loci. Comparison of GWAS results across the five locations enabled us to identify common and different signals of trait-associated genes in different environments (Figure 1C). For example, a signal was present in four locations but not in Henan for the flowering gene *ZCN8* (*Zea mays CENTRORADIALIS8*), but we detected signals for *ZCN4*

and *ZmMADS69* only in Jilin and Liaoning, respectively. GWAS for PH produced two peaks, with *BRASSINOSTEROID-DEFICIENT DWARF1* (*BRD1*) present at all five locations and *Brachytic2* (*BR2*) showing a significant peak only in Hebei and Liaoning. These results indicate that genotypes of a given gene can have conditional effects in certain environments, implying that phenotypic plasticity may result from genotype–environment interactions (i.e., how a genotype responds to the environment).

Defining environmental indexes and critical windows

Multiple environmental factors influence plant development, but their effects are too complex to consider all together in a single genotype-by-environment interaction model. Therefore, it is important to use a meaningful dimensionality reduction method to generate a unified index summarizing the underlying factors that contribute most to phenotypic plasticity. Light and temperature are two such critical ecological factors and are relatively stable in a fixed environment compared with other factors. Light intensity determines the total amount of light energy (radiant energy) that can be converted into chemical energy, and temperature determines the transformation rate of heat energy (thermal energy). Therefore, the ecological ranges for the major maize cultivation zones are usually delineated by accumulated temperature zones (ATZs), which mainly consider day length (DL) and temperature during the maize growth period from 0–120 days (17 weeks) after sowing (Supplemental Figure 2). The five locations used in this study represent the five major ATZs in China, thus providing a reference for how phenotypic plasticity may influence the selection of optimal ATZs for novel maize varieties. We first selected three environmental indexes that are commonly used in maize cultivation to model the relationship between phenotypes and the environment: growing degree days (GDDs), photothermal time (PTT), and photothermal ratio (PTR). PTT and PTR are the product and ratio between DL and GDD, respectively, which summarize the contribution of radiant energy (light) and thermal energy (temperature) to maize development in single metrics (Robertson, 1968; Fischer, 1985; Masle et al., 1989; Liu and Heins, 2002; Ravi Kumar et al., 2009; Wilczek et al., 2009). For PTT and PTR, we used the real DL (monitored in real time) instead of the theoretical DL (based on latitude). This is because the real DL represents the actual duration of light received by the plant during the day and better reflects the real photosynthetic energy (Supplemental Figure 2). We then determined the critical window of maize development during which each phenotype showed the strongest positive association with the three indexes, followed by selection of a representative index for subsequent model construction. Identifying critical growth periods during which crops are sensitive to environmental stimuli helps to quantify the effect of environmental dimensions on phenotypes. We therefore calculated all possible values for GDD, PTT, and PTR in any time window within the time range of 0–60 days after sowing using weather data collected at the five locations (methods). We then computed a series of correlations between the three phenotypes and the three indexes within any time window before generating the corresponding correlation heatmaps (Figure 2A and Supplemental Figure 3). The heatmaps provided a visual means to easily identify the time windows with the strongest correlations between phenotypes and indexes, which we defined as critical windows (methods). These windows indicate the stage for expression of a trait during which the environment has the greatest influence on phenotypic plasticity. Taking GDD as an example, the critical windows for FT, PH, and EW in inbred lines were 11–36, 37–46, and 47–54 days, respectively (Figure 2B). Although we obtained different critical windows when traits and indexes varied, we observed no significant differences between inbred and hybrid lines.

The correlations between phenotypes and environmental indexes show that environmental changes (Supplemental Figures 1 and 4), such as longer DLs and lower temperatures with increasing latitude as represented by the five ATZs (Supplemental Figure 2), appear to have a linear effect on phenotypic changes in FT, PH, and EW. In addition, the different critical windows for average GDD, PTT, and PTR for each trait indicate that sensing of light and temperature at different vegetative growth stages may make different contributions to phenotypic effects, as exemplified by the three critical windows for EW (GDD, 47–54 days; PTT, 26–35 days; PTR, 15–24 days). This phenomenon of correlated environmental change and phenotypic variation was defined as PPRE, which we then examined through statistical modeling.

Biological implications of the parameters in the PPRE model

Taking FT as an example, we determined that the average FT values of inbred, hybrid, and tester lines exhibited linear correlations with all three indexes (within the critical window period) across the five locations (Supplemental Figure 4A). Therefore, a simple linear model may effectively describe how phenotypic plasticity responds to the environment in maize. FT was negatively correlated with GDD when plotted as a function of latitude, but FT was positively correlated with PTT and PTR. We reasoned that the three correlations describe the same relationship between FT and the environment. FT was gradually delayed across the five ATZs from low to high latitudes, reflecting the need for longer days at high latitudes and low temperatures than at low latitudes and high temperatures in order to accumulate sufficient biomass during the vegetative phase before the transition to the reproductive stage. Low temperatures decrease the rate of GDD accumulation but not the accumulated degree days required for flowering. Of the three indexes, PTR showed the highest correlations with FT, as evidenced by the distribution of the correlations between PTR across all 1404 inbred lines (Supplemental Figure 4B). We therefore selected PTR as the representative index for constructing the PPRE model for the three traits and performed GWAS analysis. In the subsequent analysis of the PH model parameters, we found that the PTT index better represented the effect of the environment on PH, and we then used PTT for genomic prediction and parental plasticity analysis of PH.

The PPRE model may be simply formulated by the linear model $Y_{ij} = a_i + b_i \times X_j$, where Y_{ij} is the phenotypic value of sample i in location j, and X_j is the value of the environmental index in location j. The PPRE model was defined from an applied perspective, and it effectively explains the linear relationship between each phenotype (FT, PH, and EW) and the PTR index

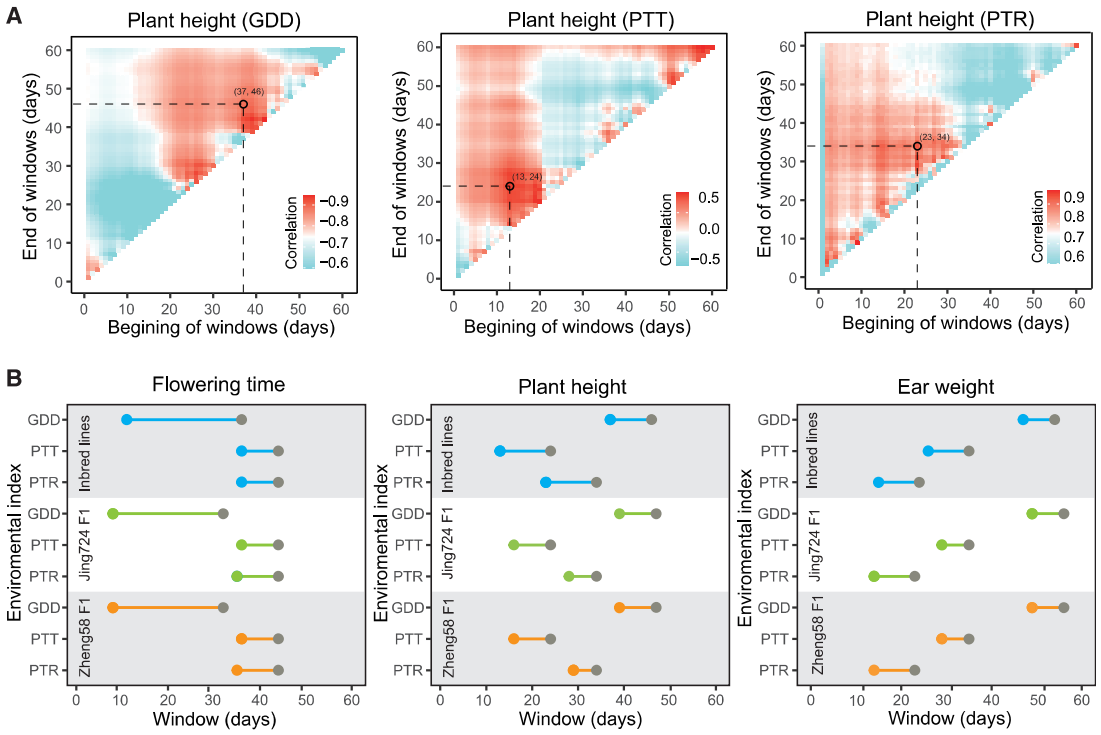

Figure 2. Determination of the correlated environmental index and the critical window for vegetative growth.

Heatmaps of the correlations between phenotypes and indexes show the critical time windows with the strongest correlations, indicating the critical stage during development when the environment has the greatest influence on the phenotypic plasticity of a given trait.

(A) Heatmaps of the correlations between three environmental indexes (any time window within the time range of 0–60 days) and the PH phenotypic mean of the inbred population. Circles on the heatmaps represent the selected critical window periods.

(B) Critical window periods for population trait–environmental index combinations. The critical window period for a given trait and environmental index was similar across different maize populations.

(Figure 3A). In the PPRE model, intercept *a* and slope *b* are the only two reaction norm parameters. Placing these two parameters in a biological context helps to clarify the genetic mechanism underlying the model. Intercept *a* may be interpreted as the phenotypic variant contributed by the genotype of a sample per se (*G*) in environment (*E*), expressed as (*G*+*E*), which reflects the performance per se in the average environment among those sampled. Slope *b* represents the extent of the contribution by the same genotype (*G*) in response to different environments (*E*), manifested as *G*×*E*, and reflects the rate of change in performance per se with respect to the magnitude of deviations from the average environment. Based on the above assumptions, the absolute value of the slope, |*b*|, may be used to describe the degree of phenotypic plasticity. Taking FT as an example, as illustrated in Supplemental Figure 4A, different ways of computing environmental indexes in the same environment may be positively or negatively correlated with the same trait. Therefore, we only considered the absolute value of the intercept. The absolute value of the slope, |*b*|, may be used to describe the degree to which a given genotype responds to a designated environment. That is, the larger the value of |*b*|, the greater the plasticity this genotype will exhibit in response to a broad range of environments as an indication of adaptability. Phenotypic plasticity is often highly adaptive (Whitman and Agrawal, 2009) and provides organisms with the potential to respond rapidly and effectively to environmental change (Charmantier et al., 2008). By contrast, a small absolute value of the slope is an indication of phenotypic stability.

We obtained the values for intercept *a* and slope *b* derived from the PPRE model for all inbred lines and used them individually as traits to perform GWAS. We surmised that this approach would enable the identification of genes that contribute to phenotypic plasticity and also help to classify them based on their contributions arising from (*G*+*E*) (from the *a* GWAS) or *G*×*E* (from the *b* GWAS) effects. We used *a* and *b* derived from the PPRE model constructed based on FT and PTR (FT-PTR model) data for the GWAS across all 1404 inbred lines. We then compared these results with those obtained by GWAS on FT itself (Figure 1C). In addition to peaks around *ZmMADS69* and *ZCN8* already detected by GWAS using FT data as a trait, we observed two additional peaks that coincided with the genomic locations of *Eps15 homology domain 1* (*ZmEHD1*) and *Constans of Zea mays1* (*CONZ1*) when slope *b* was used for GWAS (Figure 3B, top panel). By contrast, we detected only one peak for *ZmMADS15* from the GWAS of intercept *a* (Figure 3B, bottom panel). Although all five of these genes participate in the regulation of FT in maize, their roles related to (*G*+*E*) or *G*×*E* effects thus appeared to be distinct. We performed the same analysis for the results obtained by GWAS for the traits PH, *a*, and *b* derived from the PH-PTR model. Although GWAS for PH

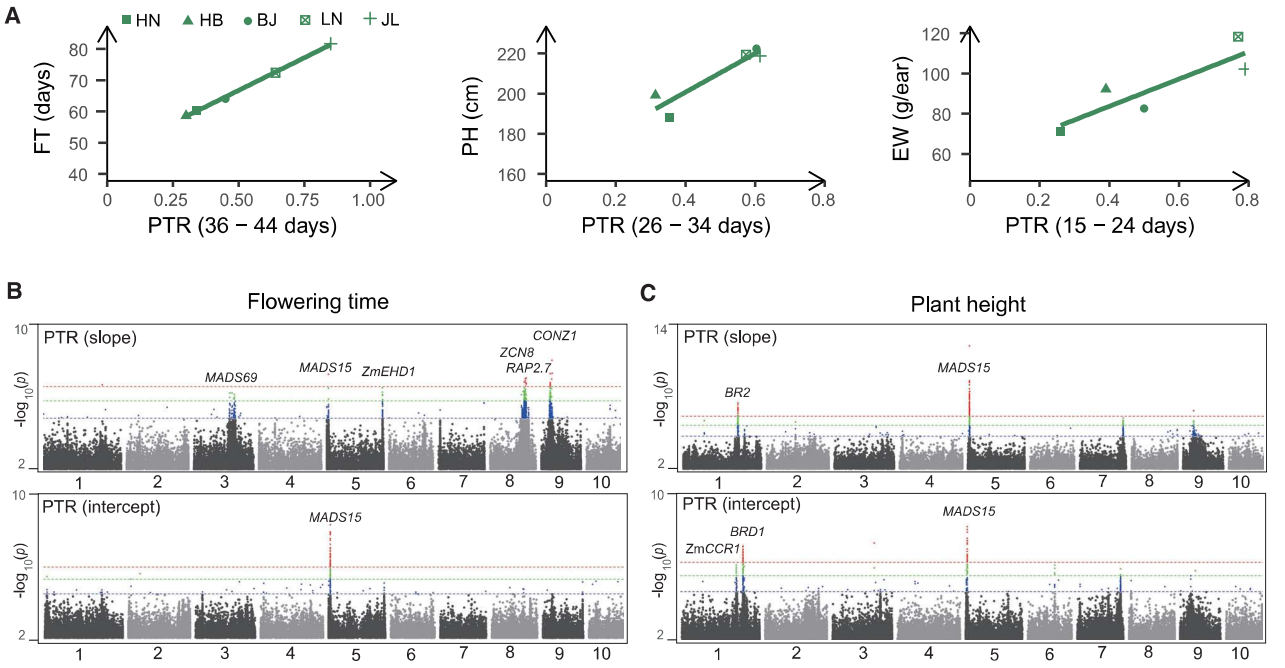

Figure 3. PPRE models and Manhattan plots from GWAS of model parameters.

(A) Phenotypes at the five locations were fitted linearly for each inbred population to the environmental index during the critical window period, and a linear model of phenotypic plasticity response to the environment (PPRE) was established. Two linear parameters were obtained for each PPRE model: intercept *a* and slope *b*.

(B and C) Manhattan plots from GWAS on the intercept and slope values derived from FT phenotypic plasticity **(B)** and PH phenotypic plasticity **(C)** of the maternal population. Model parameters identify and differentiate endogenous signal–responsive genes ([*G*+*E*], intercept *a*, bottom) and environmentally sensitive genes (*G*×*E*, slope *b*, top) that contribute to phenotypic plasticity.

identified genomic regions containing *BRD1* and *BR2* simultaneously, GWAS for *a* detected only *BR2*, and GWAS for *b* detected only *BRD1* (Figure 3C). We also obtained two additional peaks not seen in the GWAS results for PH: one peak at *ZmMADS15* using *b* as the trait and one at *Cinnamoyl-coenzyme A reductase 1* (*ZmCCR1*) using *a* or *b* as the trait. Collectively, these results indicate that genes associated with FT and PH play different roles in phenotypic plasticity through different effects of (*G*+*E*) or *G*×*E*, which will be addressed in the discussion.

Linear parameters from the PPRE model assist in genomic predictions

Genomic prediction using a GS model has been widely used to reduce phenotyping costs associated with large-scale field trials. The most widely used GS method is the ridge regression best linear unbiased prediction (rrBLUP) model, which usually directly predicts the BLUP value of the phenotypes (Heffner et al., 2009; Guo et al., 2012; Massman et al., 2013). To describe the performance of complex traits in multiple environments, linear parameters derived from the PPRE model can be used as intermediate targets for phenotypic predictions. Li et al. (2018) and Guo et al. (2020) developed the method for prediction of phenotypic plasticity model parameters and confirmed the reliability of model parameter predictions (Li et al., 2018; Guo et al., 2020). Here, we used four methods to predict the phenotypes of inbred lines under four distinct scenarios (Figure 4A) and compared the cost and prediction accuracy of the four methods (Figure 4B).

Method 1 (M1) uses the phenotypes collected in the four environments to 1) build a PPRE model, 2) calculate the intercept *a* and slope *b* of each line, and 3) calculate the phenotypic value according to the environmental index of the fifth environment to be tested/predicted. Thus, M1 predicts phenotypes in untested environments using 80% of all phenotypes collected and 80% of the associated cost (relative to phenotyping the entire panel), but there is no cost for genotyping. M1 is suitable when testing ecoregions with small sample sizes (e.g., candidate varieties), and its predictive effect is the upper limit of phenotypic prediction.

Method 2 (M2) uses the rrBLUP method (methods) to predict phenotypes from genotypes. In this case, the genotypic data of inbred lines were randomly and evenly split into a training set and a test set 10 times. M2 is useful for predicting the phenotype of untested genotypes in tested environments; this approach requires 50% of the phenotyping cost and 100% of the sequencing cost. The predictive effect of M2 is optimal for predicting phenotypes from genotypes.

Method 3 (M3) takes the linear parameters *a* and *b* as intermediate targets for prediction. The inbred lines were randomly but equally separated into training and test sets (50:50). First, a PPRE model of the training set is established using phenotypic and environmental data at all five locations to derive the model parameters (intercept *a* and slope *b*). The model parameters of the test sets are then predicted using the rrBLUP method described above. The predicted parameters and environmental

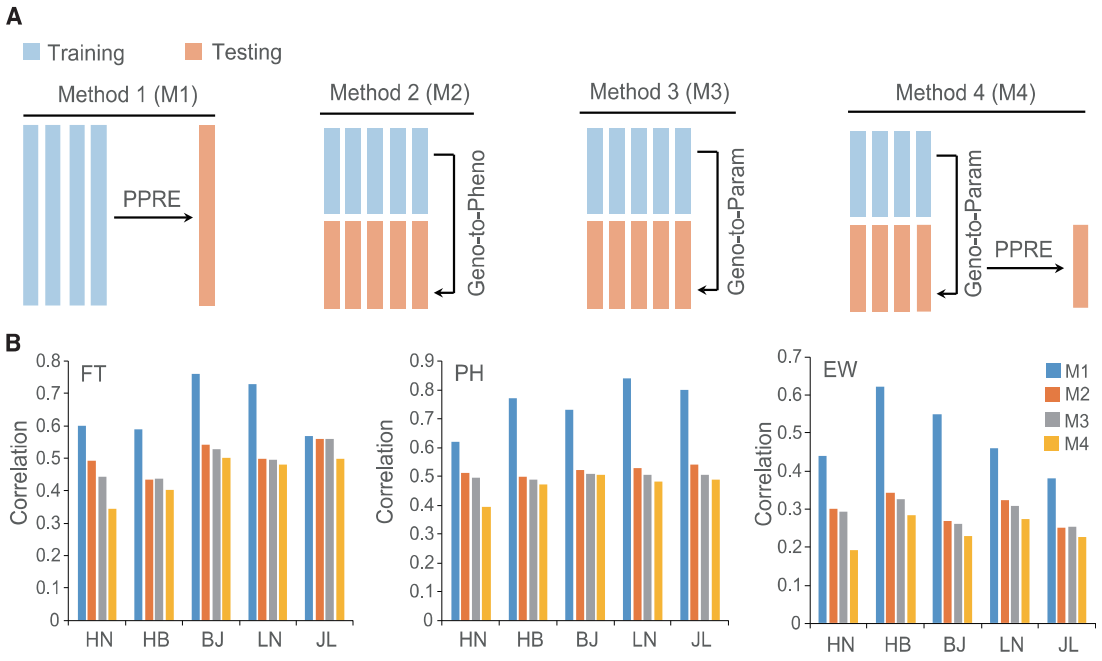

Figure 4. Linear parameter–assisted genomic prediction.
(A) Schematic of the four genome prediction methods. Method 1 (M1) uses the parameters of the PPRE model to predict phenotypes in untested environments. M2 uses the rrBLUP method to predict the phenotypes of untested genotypes in tested environments. M3 and M4 use model parameters as intermediate targets to predict the phenotypes of untested genotypes in tested environments and untested environments, respectively.
(B) Accuracy of the four genome prediction methods for three traits in the inbred population, i.e., Pearson's correlation coefficients between predicted and observed values.

indexes are used to calculate the phenotypes of the test sets. M3 predicts the phenotypes of untested genotypes in tested environments and requires 50% of the phenotyping cost and 100% of the genotyping cost. M3 costs almost the same as M2, and it forecasts similar effects as M2. The advantage of M3 compared with M2 is that the model parameters of M3 can be used to predict phenotypes from other environments.

Method 4 (M4) also uses linear parameters as intermediate targets for prediction but is based on the PPRE model established from data for four of the five environments. The phenotypic values are then calculated based on the environmental index of the target environment. M4 is suitable for predicting phenotypes of untested genotypes in untested environments and requires 40% of the phenotyping cost and 100% of the genotyping cost. M4 predicts the most challenging scenarios with acceptable forecast accuracy, and the total cost is further reduced.

Predictive model parameters can therefore assess the performance of genetically complex lines grown in multiple environments. Based on the model parameters of a given trait, crop germplasm better adapted to specific environments (ecoregions) can be selected, thereby facilitating large-scale planting, pollination, and harvesting. It is a given that the larger the training set, the greater the possible benefits. However, we need to focus on and compare the prediction accuracy of different methods and discuss the balance of acceptable costs and benefits in the breeding process.

The concordant response of biparental lines influences hybrid performance

It has been reported previously that the environment may affect hybrid performance in maize (Munaro et al., 2011; Blum, 2013). Because *a* and *b* from the PPRE model can statistically describe the *G*×*E* interaction, we sought to determine whether the concordance of *a* and *b* parameters from the two parental lines of a cross is correlated with the extent of hybrid performance. We used another previously published dataset of 6210 F_1 hybrids generated by crossing 207 CUBIC lines as maternal lines with 30 paternal tester lines (Liu et al., 2020). We measured the same three phenotypes (FT, PH, and EW) in the same five locations. Because the 30 tester lines were selected from different heterotic groups, the GCA values calculated from the EW of their F_1 offspring covered a different range (Supplemental Table 1). Twenty-seven testers had available FT-PTR model parameters because three lines had missing FT data. We ranked all 27 tester lines by their GCA values and classified them into three groups with high, moderate, or low GCA. As with the inbred population, we determined the critical windows and constructed the PPRE model separately for the maternal and paternal lines (methods), resulting in a set of *a* and *b* values from each FT-PTR model. We then generated a scatterplot, plotting the slope *b* along the x axis and the intercept *a* along the y axis for the maternal lines (Figure 5A, top left panel). We observed a negative correlation between *a* and *b* ($y = -0.77x + 70.6$), illustrating how FT of the maternal population responds to the environment as represented by the PTR index. We generated corresponding scatterplots for the three groups of

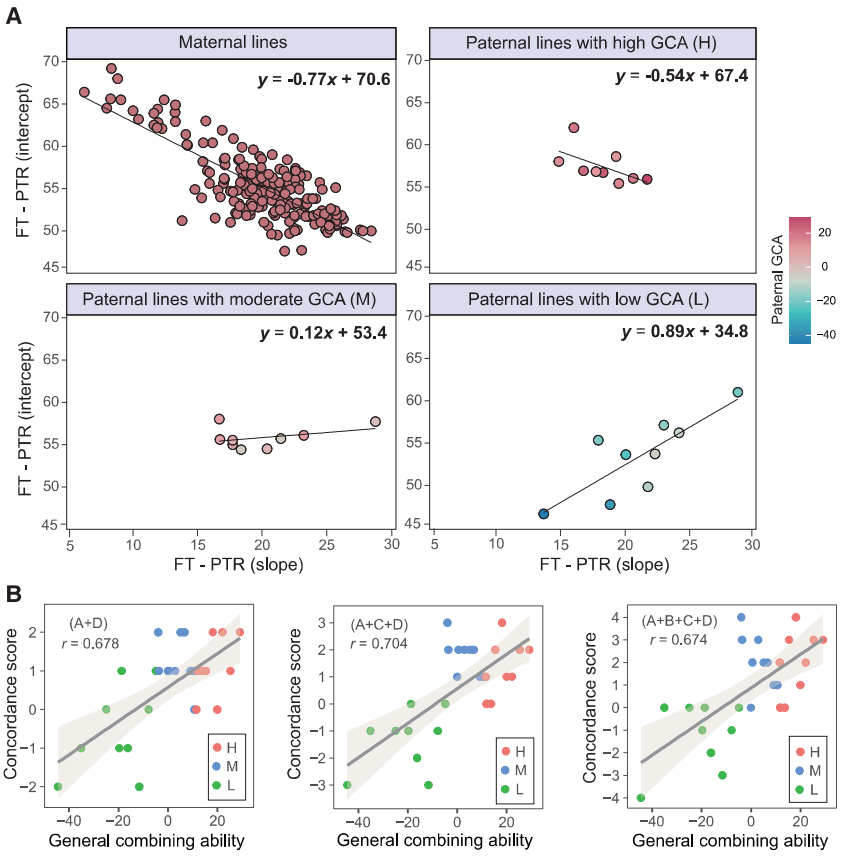

Figure 5. The concordant response in biparental lines influences hybrid performance.
(A) Scatterplots of model parameters derived from the FT-PTR model of 207 maternal (left) and 30 paternal (right) lines. The slope and intercept values are plotted along the x axis and y axis, respectively. For testers with high general combining ability (GCA), the regression line is approximately parallel to the regression line of the maternal population, and the distribution is closest to the center of the maternal population.
(B) Scatterplots of model parameter concordance scores and GCAs of the tester lines. The concordance scores were normalized and graded from differences between the four model parameters between the paternal and maternal lines.

paternal testers. For testers with high GCA, the regression line ($y = -0.54x + 67.4$) was approximately the same as that of the maternal population (Figure 5A, top right panel), with an overall distribution closest to the center of the maternal population. Regression lines for testers with moderate and low GCA ($y = 0.12x + 53.4$ and $y = 0.89x + 34.8$, respectively) showed trends opposite to that of the maternal population (Figure 5A, bottom right panel), and the distribution of individual points was more scattered and farther from the center of the maternal population. The similar regression lines of maternal lines and paternal lines with high GCA suggested that the extent of hybrid performance may be correlated with the extent of biparental concordance for environmental response. In other words, the FTs of inbred lines from two heterotic groups must respond concordantly to the environment to produce ideal yield heterosis in their derived F_1 hybrids.

If the above hypothesis is correct, then a PPRE model may be sufficient to derive parameters *a* and *b* and perform an initial evaluation of hybrid performance, given two populations of inbred lines, without the need to generate or phenotype F_1 hybrids. High-yielding F_1 hybrids would be expected for maternal and paternal lines with similar *a* and *b* parameters, which can be estimated by their closeness in values. Because both FT and PH were correlated with EW, we focused on the FT-PTR and PH-PTT models. Using the resulting *a* and *b* values, we subtracted the paternal *a* (or *b*) value from the averaged *a* (or *b*) value of the maternal population before applying a normalization by score to describe the closeness of biparental concordance, resulting in four descriptive scatterplots (methods). They are differences of biparental (A) FT-PTR model intercept *a*, (B) FT-PTR model slope *b*, (C) PH-PTT model intercept *a*, and (D) PH-PTT model slope *b* (Supplemental Figure 5). We detected a significant correlation between intercept *a* derived from the FT-PTR model (A) and paternal GCA values ($r = -0.459$, $P = 0.016$) and between slope *b* from the PH-PTT model (D) and paternal GCA values ($r = -0.612$, $P = 0.001$). When we added the scores from models A and D, we observed an increase in the final concordance score ($r = 0.678$, $P = 7.24 \times 10^{-5}$) with paternal GCA (Figure 5B). Adding the score from model C to those from models A and D further improved precision ($r = 0.704$, $P = 2.93 \times 10^{-5}$). In summary, the above analysis validated our hypothesis that biparental concordance in environmental response is likely necessary for achieving ideal heterosis (high combining ability) between two inbred lines. This result may offer a convenient and low-cost means of interrogating GCA without having to generate or phenotype F_1 hybrids.

The response of parental phenotypic plasticity to the environment affects combining ability

We next explored the effect of biparental PPRE on heterosis. To this end, we determined the critical windows and constructed a PPRE model for FT-PTR and PH-PTT, from which we derived intercept *a* and slope *b* for the 207 maternal lines. We plotted scatterplots of the 207 maternal model parameters with their GCA values, and there appeared to be a positive correlation between the maternal model parameters and their GCA values (Supplemental Figure 6). To quantify this relationship and facilitate decision making, we classified maternal lines into five classes based on the magnitude (absolute value) of the model parameters and calculated the corresponding changes in maternal GCA values (Supplemental Table 2; Figure 6A). We determined that larger FT-PTR slope values in the maternal line were associated with higher GCA values. Likewise, a greater PH-PTT intercept value in the maternal line coincided with a higher GCA value, that is, the environmental plasticity of parental

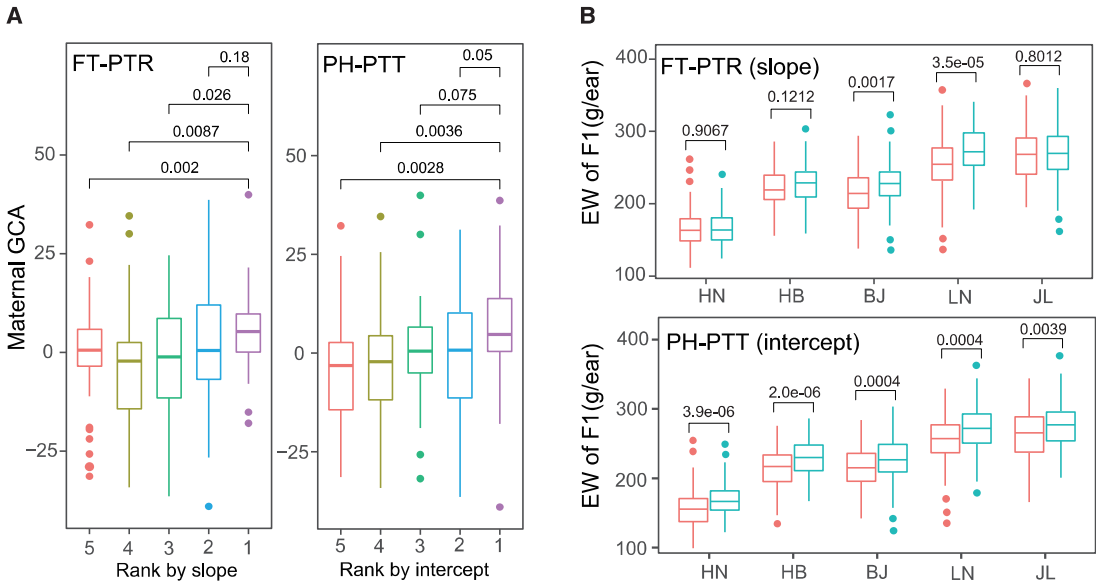

Figure 6. The response of parental phenotypic plasticity to the environment affects hybrid performance.

(A) Boxplots of the relationship between 207 maternal model parameters and their GCA values. The x axis indicates the ranking of 207 maternal lines according to the magnitude (absolute value) of the model parameters, and the y axis indicates their corresponding GCA values. The values above the boxes are the *P*values of the differences between the two sets of maternal GCA data calculated using the t-test method.

(B) Boxplots of the relationship between 1404 maternal model parameters and the yields of their F_1 hybrids from crosses with Zheng58 in different locations. The x axis indicates the model parameters in the different locations, showing the bottom 10% (left) and the top 10% (right). The y axis indicates the EW of each Zheng58 F_1 hybrid. The values above the boxes are *P*values calculated using the t-test method for differences between the EWs of hybrids produced by the two maternal groups with the bottom 10% and top 10% model parameters.

FT (*G*×*E*) and the performance of parental PH in the environment (*G*+*E*) positively affected its GCA.

To verify this idea, we derived intercept *a* and slope *b* from the FT-PTR and PH-PTT models for the 1404 maternal lines. We generated a scatterplot (Supplemental Figure 7) and colored the points using the EW values corresponding to the F_1s. The model parameters of the maternal line appeared to distinguish the high- and low-yielding F_1s. To perform statistical tests to determine the significance level of the difference between the two groups, we separated the maternal lines into the bottom 10% and top 10% based on each model parameter value, thus defining two sets of 140 maternal lines. We then extracted EWs for their corresponding F_1 hybrids when crossed to Zheng58 and plotted the values as boxplots at each of the five locations (Figure 6B). We obtained results that were largely consistent with the above hypothesis and observed that the differences in EW between the bottom 10% (left) and top 10% (right) groups were not uniform across locations. Indeed, the FT-PTR for slope was significantly different between the two groups at two locations, Beijing and Liaoning, and the PH-PTT for intercept was significantly different at all five locations. At the same time, when the maternal lines were crossed to Jing724, we extracted the EWs of their corresponding F_1 hybrids (Supplemental Figure 8) and found the same pattern. FT-PTR for slope was significantly different between the two groups at three locations, and PH-PTT for intercept was significantly different at four locations. In Figure 6B and Supplemental Figure 8, it can be seen that the EWs of the two F_1 populations were in multiple locations, a total of 20 sets, showing the same pattern at the same time; that is, the bottom 10% (left) of EW for F_1 is lower than the top 10% (right). These differences were significant in 14 of the sets. This observation suggests that the extent to which parental phenotypic plasticity affects hybrid performance (high yield) depends on the environment.

Based on PPRE model parameters and their biological meanings, we revealed how parental FT and PH affect combining ability, thus producing positive hybrid performance that is environmentally dependent. We established that strong phenotypic plasticity in the parents results in higher yield for the corresponding hybrid. Varieties with greater plasticity may therefore support high yields in multiple and varied environments. Selection of hybrids with high adaptability and plasticity should thus be a key goal of maize breeding.

DISCUSSION

We obtained the linear model of PPRE by fitting phenotypic values against an environmental index in multiple ecoregions. This model can be used to describe the phenotypic change in a given inbred or hybrid line attributable to changes in the environment. It is simply formulated by the linear model $Y_{ij} = a_i + b_i \times X_j$, where Y_{ij} is the phenotypic value of sample *i* in location *j*, and X_j is the environmental index in location *j*. The parameter *a* is the intercept of the regression line with the y axis and is the expected value of *Y* when $X = 0$. The parameter *b* is the slope of the regression line, called the regression coefficient, and represents the average change in *Y* when *X* changes by one unit. It should be noted that $X = 0$ in the linear model is a statistical theoretical

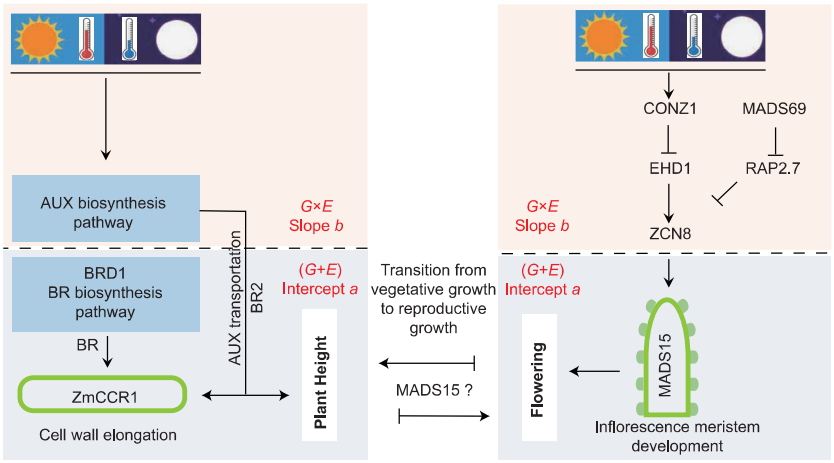

Figure 7. Genetic regulatory pathways control flowering and PH in response to light and heat.
Top panel: environmentally sensitive genes (class B) detected by slope *b*. Bottom panel: endogenous signal–responsive genes (class A) detected by intercept *a*. Left panel: genetic regulatory pathway for PH involving the identified genes. Right panel: genetic regulatory pathway for FT. Together, class A and B genes contribute to the phenotypic plasticity of an individual in response to the environment. Coordinated regulation of the two classes of genes controlling flowering and PH in the F1 hybrid genome may be the basis for high yield.

case, such as GDD below the base temperature or direct solar irradiance below 120 W/m^2 throughout the day (methods), and the environmental index is always recorded as 0, with no negative values. In the case of $X = 0$, only genotypic effects are considered, representing the contribution of genes that are responsive to endogenous signals. Autonomous flowering, for example, is not affected by exogenous signals such as light or temperature.

Phenotypic plasticity is shaped by the genotype of an individual in the environment (*G*+*E*) in addition to the interaction effect between the genotype and the environment (*G*×*E*). In the PPRE model, intercept *a* represents (*G*+*E*), emphasizing the phenotypic variance contributed by the genotype of an individual per se, whereas slope *b* represents *G*×*E*, or the contribution of a genotype in response to different environments. The biological implications of *a* and *b* may then be explained by two sets of genes involved in sensing endogenous developmental signals or exogenous environmental signals, respectively. In addition, because *a* and *b* describe the extent of phenotypic plasticity of each individual, they can also be treated as individual traits for GWASs to identify their respective causal loci and describe the biological mechanisms underlying phenotypic plasticity.

Maize is one of the most widely cultivated crops in the world, largely because of its diverse FTs in various environments (Liang et al., 2019). Much of our knowledge about the factors that control FT comes from research on the model plants *Arabidopsis thaliana* and rice (*Oryza sativa*) (Shrestha et al., 2014; Blümel et al., 2015). By contrast, less is known about the genetic control of FT in maize, especially for genes involved in the transition from vegetative to reproductive growth. GWASs using parameters *a* and *b* derived from the FT-PTR and PH-PTR models identified genes previously found by GWASs using FT and PH as traits but also revealed new candidate genes not revealed by GWASs with these classic traits. Importantly, GWASs using *a* and *b* enabled us to classify these candidate genes into two classes (Figure 3B and 3C). Class A contains genes that determine phenotypes by (*G*+*E*) per se in response to endogenous developmental signals, whereas class B contains genes that shape phenotypes by *G*×*E* in response to exogenous environmental signals. The relationship between the two classes of genes derived from the FT-PTR and PH-PTR models may facilitate a better understanding of the mechanisms that underlie phenotypic plasticity (Figure 7).

Physiological studies in *Arabidopsis* have shown that the florigen *FLOWERING LOCUS T* is a mobile factor that transmits floral inductive signals from the leaves to the shoot apex (Zeevaart, 2008). The maize *FLOWERING LOCUS T*ortholog *ZCN8* integrates endogenous and photoperiod flowering signals (Lazakis et al., 2011). From the inbred population, the GWAS of slope *b* derived from the FT-PTR model detected a signal at *ZCN8* but also near the genes *CONZ1*, *ZmEHD1*, *ZmMADS69*, and *Related to AP2.7* (*ZmRAP2.7*), indicating that this class of genes forms a regulatory module that senses environmental signals, such as changes in photoperiod, to determine FT. In this module, the *CONZ1-ZmEHD1-ZCN8* (Miller et al., 2008; Xiao et al., 2021) and *ZmMADS69-ZmRAP2.7-ZCN8* pathways have been reported to control FT and contribute to photoperiod adaptation (Liang et al., 2019). The above observations support the notion that the GWAS of *b* can detect environmentally sensitive genes and reveal the molecular mechanisms by which *G*×*E* influences phenotypic plasticity variation. By contrast, the GWAS of *a* detected *ZmMADS15*, which was previously reported as a floral meristem identity gene involved in floral induction and inflorescence development (Danilevskaya et al., 2008). These results are consistent with the idea that intercept *a* represents one or more factors responsive to endogenous developmental signals, revealing the biological role of (*G*+*E*) in phenotypic plasticity.

Similarly, the GWAS of *a* and *b* derived from the PH-PTR model detected two classes of genes contributing to PH. The GWAS of *b* detected a signal for *BR2*, which encodes a polar transporter of auxin; this phytohormone regulates light-induced cell elongation through its effect on cell wall modifications (Masuda, 1990). The GWAS of *a* identified signals at the *BRD1* and *ZmCCR1* loci, which encode enzymes responsible for brassinosteroid and lignin biosynthesis, respectively (Tamasloukht et al., 2011; Makarevitch et al., 2012). Therefore, *BR2* represents the *G*×*E* effect through sensing exogenous environmental signals,

whereas *BRD1* and *ZmCCR1* represent the effect of (*G*+*E*). This finding is consistent with a previous report that the auxin and brassinosteroid pathways often act synergistically to regulate cell elongation and cell proliferation (Hardtke et al., 2007). Interestingly, we also detected a *ZmMADS15* signal during GWAS for both parameters. This result indicates that *ZmMADS15* may play an intermediate role in coordinating the transition from vegetative to reproductive stages during floral initiation.

In this work, we established a linear model that describes PPRE and applied it to three representative traits: FT, PH, and EW. Using the two main parameters of the linear model, slope *b* and intercept *a*, we interpreted the biological implication of phenotypic plasticity and identified key genes based on their contributing effects for *G*×*E* and (*G*+*E*), respectively. We further demonstrated that F_1 hybrids with high yields tended to be characterized by concordant plasticity in the phenotypes of their two parental lines, suggesting a relationship between hybrid performance and biparental plasticity. This relationship suggests that the basis for formation of combining ability between different heterotic groups may depend on the consistency of the regulatory pathways to which class A and class B genes belong in the biparental genomes. That is, greater regulatory consistency between the two sets of genes from biparental lines will result in a higher combining ability in their corresponding hybrid. Therefore, phenotypic plasticity essentially reflects the regulatory concordance of the two classes of genes. To ascertain whether the above rules can be applied to precision breeding, we developed a scoring method that uses the two parameters from the linear model to select inbred lines and predict the performance of their F_1 hybrids. Indeed, F_1 hybrids derived from a cross between inbred lines with high scores showed superior performance. This result supports theoretical and empirical studies suggesting that selection of phenotypic plasticity can result in adaptation to different environmental conditions (Via and Lande, 1985; De Jong, 2005). Varieties with greater plasticity can therefore sustain high and stable yields in multiple environments. We conclude that the identification of varieties with high indexes of adaptability and plasticity may be valuable for selection and practical use.

METHODS

Germplasm and phenotyping

We used four previously published maize populations: one inbred population and three hybrid populations. The inbred population consisted of CUBIC lines containing 1404 lines used as the maternal pool for crossing with paternal tester lines. The first hybrid population contained 6210 F_1 hybrids generated by crossing 207 maternal lines with 30 paternal testers. The other two hybrid populations were two sets of F_1 hybrids generated by crossing 1404 maternal lines with two elite testers, Jing724 and Zheng58. All lines were planted in 2014 in five locations (N 35°31′, E 113°85′, Xinxiang City, Henan Province; N 38°85′, E 115°48′, Baoding City, Hebei Province; N 40°13′, E 116°13′, Shunyi District, Beijing City; N 41°48′, E 123°38′, Shenyang City, Liaoning Province; N 43°88′, E 125°35′, Changchun City, Jilin Province) in northern China (Supplemental Table 3). The planting-to-harvest dates for the five locations were June 10 to October 16 (169 days), May 29 to October 6 (159 days), May 12 to September 29 (152 days), May 11 to October 2 (155 days), and May 9 to October 19 (172 days). The experiment used a randomized complete block design with 20 inbred lines or hybrids planted in each row in the field. Three replications of each line were planted and randomly sampled for measurement. Three phenotypes were measured: FT (measured as the interval from sowing to the day the tassel appeared in half of the individuals per line), PH (vertical height from the ground to the top of the tassel with an accuracy of 0.5 cm), and EW (Supplemental Table 4). The GCA values of 30 paternal lines and 207 maternal lines (Supplemental Table 1; Supplemental Table 2) were calculated using the function $mmer(EW \sim Loc, random = \sim P1 + P2 + Line)$ in the "sommer" R package (Covarrubias-Pazaran, 2016), where *EW* represents the phenotypic value of EW of 6210 F_1s at five locations, and *Loc* represents the five locations as a fixed effect in the mixed linear model. The broad-sense heritability (*H*) of the three traits in the maternal population was computed using the formula $H = V_g / (V_g + V_e / L)$, with the function $lmer(Trait \sim (1|Line) + (1|Loc))$ in the R package "lme4" (Bates et al., 2014), where V_g is the genetic variance, V_e is the environmental variance, and *L* is the number of environments.

Data availability

Resequencing analysis was performed on 1404 maternal lines and 30 paternal lines. The raw sequencing reads were deposited at NCBI under BioProject accession number PRJNA597703 (https://www.ncbi.nlm.nih.gov/bioproject/PRJNA597703). A total of 6 795 498 high-quality SNPs called from whole-genome resequencing of the 1404 inbred lines were used for GWAS analysis and phenotype prediction (link to genotype data: https://github.com/furan2019/GenoData).

Environmental indexes

The meteorological data used in this study came from real-time monitoring of the meteorological base stations where the fields were located. Three environmental indexes were examined: GDD, PTT, and PTR. GDDs are used to estimate the growth and development of plants and insects during the growing season. The basic concept is that development will only occur when the temperature exceeds some minimum developmental threshold or base temperature (*Tbase*). *Tbase is* determined experimentally and is different for each organism. The *Tbase* for maize is 10°C (50°F). To calculate GDDs, the mean temperature for the day is calculated and defined as the sum of the highest (*Tmax*) and lowest (*Tmin*) temperatures for the day, divided by two. If the mean temperature is at or below *Tbase*, then the GDD value is zero. If the mean temperature is above *Tbase*, then the GDD value equals the mean temperature minus *Tbase.* Average GDD, PTT, and PTR values with different starting days with a window size from 5 to 25 d during the growing season were obtained for each environment. The average GDD was calculated using the formula $GDD = \left(\sum_{S}^{S+L}\left(\frac{1}{2}(Tmax + Tmin) - Tbase\right)\right)/L$, where *S* is the *Sth* day after planting, and *L* is the length of the window in days. *Tmax* for maize growth is 40°C (104°F). DL is the real duration of sunlight monitored in real time and according to the World Meteorological Organization, and sunshine duration during a given period is defined as the sum of the time during which direct solar irradiance exceeds 120 W/m^2. PTT is the product of GDD and DL. PTR is defined as the ratio of radiant energy (light) to thermal energy (temperature), represented in this research as the ratio of DL and GDD. These two environmental indexes add another important variable to the environment: light. The average PTT was calculated using the formula $PTT = \left(\sum_{L}^{S+L}\left(\left(\frac{1}{2} * (Tmax + Tmin) - Tbase\right) * DL\right)\right) / L$. *DL* is the real DL detected by the meteorological base station. The average PTR was calculated using the formula $PTR = \left(\sum_{S}^{S+L}\left(\frac{DL}{\frac{1}{2}*(Tmax + T\ min) - Tbase}\right)\right)/L$.

Critical windows and the PPRE model

Average GDD, PTT, and PTR values were calculated for all possible time windows from day 0 (sowing) to day 60 at the five experimental locations. The critical window resulting in the strongest correlation with the mean values of population phenotypes within the environment was identified for average GDD, PTT, and PTR. If several time windows were strongly correlated, then the critical windows were selected based on biological significance. Correlations between the three environmental indexes in the critical window and FT at the five locations were calculated, and the

index with the strongest correlation was taken as the representative index. Among these three indexes, PTR had the highest correlation with FT, and we selected PTR as the representative index for constructing the PPRE model for the three traits and performed GWAS analysis. In further model parameter analysis, we wanted to select the best representative environmental index for each trait individually to obtain the best results. For FT and EW, we again selected PTR. However, we found that the PTT index was more representative of the environmental effects on PH, and the PTT index was used for genomic prediction and parental plasticity analysis of PH. A linear regression analysis was performed using the phenotypes of each line in the five environments and the environmental index values of the five environments during the critical window using the "lm" function in R. The linear model fitted by the phenotype and environmental index constituted the PPRE model. Lines with missing phenotypic data were removed, and only lines with phenotypic data from all five locations were retained for analysis; 1256 lines remained for the inbred population. For the 30 testers, 27 lines had available FT-PTR (FT plasticity in response to the environmental index PTT) model parameters because FT data were missing for three lines, 25 lines had available PH-PTT model parameters because PH data were missing for five lines, and 27 lines had available EW-PTR model parameters because EW data were missing for three lines.

GWAS and phenotype prediction

Genome-wide efficient mixed model association (GEMMA) software was used for GWAS (Zhou and Stephens, 2012). The phenotypes of the maternal population in each environment were examined individually. The environmentally dependent size and direction of the genomic effects were also estimated. For each trait, treating the estimates of slope and intercept as two derived features, the established mixed model GWAS was performed to identify genomic regions where variation in both slope and intercept was observed between different genotypes. Four methods were used to predict the phenotype in different environments (Figure 4A). For M1, phenotypes were predicted based on environmental indexes in a fifth environment using models built from phenotypes in the other four environments. The traversal was performed until the phenotypes were predicted for all five environments. For M2, phenotypes in each environment were predicted separately. The genotype data for the inbred lines were randomly divided into training and test sets (50:50), and the phenotypes in the test set were calculated using the R package "rrBLUP" (rrBLUP method) (Endelman, 2011). The training and test sets were swapped, and all predicted values in this environment were calculated. For M3, the inbred lines were randomly divided into training and test sets (50:50), the model parameters of the inbred lines in the training set for the five environments were calculated, the model parameters of the test set were predicted using rrBLUP, and then the predicted parameters and environmental indexes were used to calculate the phenotypes of the test set. The test and training set were swapped to obtain the predicted values in all five environments. For M4, the inbred lines were randomly and equally divided into training and test sets. The model parameters of the inbred lines in the training set were calculated for the four environments, the model parameters of the test set were predicted using rrBLUP, and the predicted parameters and the fifth environmental index were used to calculate the phenotype of the test set in the fifth environment. The test and training sets were swapped, and all predicted values in the fifth environment were calculated. The traversal was performed until the phenotypes were predicted for all five environments. For M2, M3, and M4, prediction accuracy was assessed by calculating the correlation between observed and predicted values in each environment, randomly dividing the genotypes equally, and repeating this 10 times to obtain the average Pearson's correlation coefficient (r).

Model parameter concordance score

Following the determination of the critical windows and the construction of the PPRE model, intercept a and slope b were derived from the FT-PTR model and the PH-PTT model for the 207 maternal and 30 paternal lines. The parameter (a or b) for each paternal line was subtracted from the average a or b value derived from the fitted model for the maternal population, and the absolute value of the obtained difference was further normalized so that all values fell between 0 and 1. The magnitude of the difference between the biparental parameters was defined as the closeness. Four descriptive scatterplots were plotted for the closeness and GCA values of the paternal lines. The correlations between the four closeness values and the GCA values were calculated. Two cutoff values for closeness were defined. The first standard cutoff value was used to delineate the best closeness, around 0.25 (0.2–0.3), and a closeness less than this value was scored as +1. The second cutoff value delineated the worst closeness, about 0.5 (0.45–0.6), and a closeness greater than this value was scored as −1. A closeness score between the two cutoff values was set to 0. If one of the parameters of FT and PH was missing, then the missing score was temporarily recorded as 0. If the parameters for both traits were missing, then the paternal line was omitted. The definition of the standard line in these data was artificially adjusted for the best results. Correlation analysis was performed on the four concordance scores individually or cumulatively with the GCA values of paternal lines to obtain the type of concordance score that most significantly affected the GCA value.

SUPPLEMENTAL INFORMATION

Supplemental information is available at *Plant Communications Online*.

FUNDING

This work was funded by the Hainan Yazhou Bay Seed Laboratory (B21HJ0505), the Chinese Universities Scientific Fund (2022TC139), and the 2115 Talent Development Program of China Agricultural University.

AUTHOR CONTRIBUTIONS

X.W. conceived the project, R.F. analyzed the data, and X.W. and R.F. wrote the manuscript.

ACKNOWLEDGMENTS

No conflict of interest is declared.

Received: October 11, 2022
Revised: December 31, 2022
Accepted: January 10, 2023
Published: January 11, 2023

REFERENCES

Aspinwall, M.J., Loik, M.E., Resco de Dios, V., Tjoelker, M.G., Payton, P.R., and Tissue, D.T. (2015). Utilizing intraspecific variation in phenotypic plasticity to bolster agricultural and forest productivity under climate change. Plant Cell Environ. **38**:1752–1764. https://doi.org/10.1111/pce.12424.

Bates, D., Mächler, M., Bolker, B., and Walker, S. (2014). Fitting linear mixed-effects models using lme4. Preprint at arXiv. https://doi.org/10.48550/arXiv.1406.5823.

Baye, T.M., Abebe, T., and Wilke, R.A. (2011). Genotype-environment interactions and their translational implications. Per. Med. **8**:59–70. https://doi.org/10.2217/pme.10.75.

Blackman, B.K. (2017). Changing responses to changing seasons: natural variation in the plasticity of flowering time. Plant Physiol. **173**:16–26. https://doi.org/10.1104/pp.16.01683.

Blum, A. (2013). Heterosis, stress, and the environment: a possible road map towards the general improvement of crop yield. J. Exp. Bot. **64**:4829–4837. https://doi.org/10.1093/jxb/ert289.

Blümel, M., Dally, N., and Jung, C. (2015). Flowering time regulation in crops—what did we learn from Arabidopsis? Curr. Opin. Biotechnol. **32**:121–129. https://doi.org/10.1016/j.copbio.2014.11.023.

Brachi, B., Faure, N., Horton, M., Flahauw, E., Vazquez, A., Nordborg, M., Bergelson, J., Cuguen, J., and Roux, F. (2010). Linkage and association mapping of Arabidopsis thaliana flowering time in nature. PLoS Genet. **6**:e1000940. https://doi.org/10.1371/journal.pgen.1000940.

Bradshaw, A.D. (1965). Evolutionary significance of phenotypic plasticity in plants. In Advances in Genetics, E.W. Caspari and J.M. Thoday, eds. (Academic Press), pp. 115–155. https://doi.org/10.1016/S0065-2660(08)60048-6.

Charmantier, A., McCleery, R.H., Cole, L.R., Perrins, C., Kruuk, L.E.B., and Sheldon, B.C. (2008). Adaptive phenotypic plasticity in response to climate change in a wild bird population. Science **320**:800–803. https://doi.org/10.1126/science.1157174.

Chen, Z. (2013). Genomic and epigenetic insights into the molecular base of heterosis. Nat. Rev. Genet. **14**:471–482. https://doi.org/10.1038/nrg3503.

Chevin, L.-M., and Lande, R. (2015). Evolution of environmental cues for phenotypic plasticity. Evolution **69**:2767–2775. https://doi.org/10.1111/evo.12755.

Covarrubias-Pazaran, G. (2016). Genome-assisted prediction of quantitative traits using the R package sommer. PLoS One **11**:e0156744.

Danilevskaya, O.N., Meng, X., Selinger, D.A., Deschamps, S., Hermon, P., Vansant, G., Gupta, R., Ananiev, E.V., and Muszynski, M.G. (2008). Involvement of the MADS-box gene ZMM4 in floral induction and inflorescence development in maize. Plant Physiol. **147**:2054–2069.

De Jong, G. (2005). Evolution of phenotypic plasticity: patterns of plasticity and the emergence of ecotypes. New Phytol. **166**:101–118.

Des Marais, D.L., Hernandez, K.M., and Juenger, T.E. (2013). Genotype-by-Environment interaction and plasticity: exploring genomic responses of plants to the abiotic environment. Annu. Rev. Ecol. Evol. Syst. **44**:5–29. https://doi.org/10.1146/annurev-ecolsys-110512-135806.

Duvick, D.N. (2001). Biotechnology in the 1930s: the development of hybrid maize. Nat. Rev. Genet. **2**:69–74. https://doi.org/10.1038/35047587.

Endelman, J.B. (2011). Ridge regression and other kernels for genomic selection with R package rrBLUP. Plant Genome **4**:250–255.

Fischer, R.A. (1985). Number of kernels in wheat crops and the influence of solar radiation and temperature. J. Agric. Sci. **105**:447–461. https://doi.org/10.1017/S0021859600056495.

Gage, J.L., Jarquin, D., Romay, C., Lorenz, A., Buckler, E.S., Kaeppler, S., Alkhalifah, N., Bohn, M., Campbell, D.A., Edwards, J., et al. (2017). The effect of artificial selection on phenotypic plasticity in maize. Nat. Commun. **8**:1348. https://doi.org/10.1038/s41467-017-01450-2.

Gratani, L. (2014). Plant phenotypic plasticity in response to environmental factors. Adv. Bot. **2014**:1–17. https://doi.org/10.1155/2014/208747.

Guo, T., Mu, Q., Wang, J., Vanous, A.E., Onogi, A., Iwata, H., Li, X., and Yu, J. (2020). Dynamic effects of interacting genes underlying rice flowering-time phenotypic plasticity and global adaptation. Genome Res. **30**:673–683.

Guo, Z., Tucker, D.M., Lu, J., Kishore, V., and Gay, G. (2012). Evaluation of genome-wide selection efficiency in maize nested association mapping populations. Theor. Appl. Genet. **124**:261–275. https://doi.org/10.1007/s00122-011-1702-9.

Hardtke, C.S., Dorcey, E., Osmont, K.S., and Sibout, R. (2007). Phytohormone collaboration: zooming in on auxin–brassinosteroid interactions. Trends Cell Biol. **17**:485–492. https://doi.org/10.1016/j.tcb.2007.08.003.

Heffner, E.L., Sorrells, M.E., and Jannink, J.-L. (2009). Genomic selection for crop improvement. Crop Sci. **49**:1–12. https://doi.org/10.2135/cropsci2008.08.0512.

Kelly, S.A., Panhuis, T.M., and Stoehr, A.M. (2012). Phenotypic plasticity: molecular mechanisms and adaptive significance. Compr. Physiol. **2**:1417–1439. https://doi.org/10.1002/cphy.c110008.

Kusmec, A., de Leon, N., and Schnable, P.S. (2018). Harnessing phenotypic plasticity to improve maize yields. Front. Plant Sci. **9**:1377. https://doi.org/10.3389/fpls.2018.01377.

Kusmec, A., Srinivasan, S., Nettleton, D., and Schnable, P.S. (2017). Distinct genetic architectures for phenotype means and plasticities in Zea mays. Nat. Plants **3**:715–723. https://doi.org/10.1038/s41477-017-0007-7.

Larcher, W. (2003). Physiological Plant Ecology: Ecophysiology and Stress Physiology of Functional Groups (Springer Science & Business Media).

Lazakis, C.M., Coneva, V., and Colasanti, J. (2011). ZCN8 encodes a potential orthologue of Arabidopsis FT florigen that integrates both endogenous and photoperiod flowering signals in maize. J. Exp. Bot. **62**:4833–4842. https://doi.org/10.1093/jxb/err129.

Li, X., Guo, T., Mu, Q., Li, X., and Yu, J. (2018). Genomic and environmental determinants and their interplay underlying phenotypic plasticity. Proc. Natl. Acad. Sci. USA **115**:6679–6684. https://doi.org/10.1073/pnas.1718326115.

Li, X., Guo, T., Wang, J., Bekele, W.A., Sukumaran, S., Vanous, A.E., McNellie, J.P., Tibbs-Cortes, L.E., Lopes, M.S., Lamkey, K.R., et al. (2021). An integrated framework reinstating the environmental dimension for GWAS and genomic selection in crops. Mol. Plant **14**:874–887. https://doi.org/10.1016/j.molp.2021.03.010.

Liang, Y., Liu, Q., Wang, X., Huang, C., Xu, G., Hey, S., Lin, H.-Y., Li, C., Xu, D., Wu, L., et al. (2019). ZmMADS69 functions as a flowering activator through the ZmRap2.7-ZCN8 regulatory module and contributes to maize flowering time adaptation. New Phytol. **221**:2335–2347. https://doi.org/10.1111/nph.15512.

Liu, B., and Heins, R. (2002). Photothermal ratio affects plant quality in 'Freedom' Poinsettia. J. Am. Soc. Hortic. Sci. **127**:20–26. https://doi.org/10.21273/JASHS.127.1.20.

Liu, H.-J., Wang, X., Xiao, Y., Luo, J., Qiao, F., Yang, W., Zhang, R., Meng, Y., Sun, J., Yan, S., et al. (2020). CUBIC: an atlas of genetic architecture promises directed maize improvement. Genome Biol. **21**:20. https://doi.org/10.1186/s13059-020-1930-x.

Makarevitch, I., Thompson, A., Muehlbauer, G.J., and Springer, N.M. (2012). Brd1 gene in maize encodes a brassinosteroid C-6 oxidase. PLoS One **7**:e30798.

Malosetti, M., Ribaut, J.-M., and van Eeuwijk, F.A. (2013). The statistical analysis of multi-environment data: modeling genotype-by-environment interaction and its genetic basis. Front. Physiol. **4**:44. https://doi.org/10.3389/fphys.2013.00044.

Masle, J., Doussinault, G., Farquhar, G.D., and Sun, B. (1989). Foliar stage in wheat correlates better to photothermal time than to thermal time. Plant Cell Environ. **12**:235–247. https://doi.org/10.1111/j.1365-3040.1989.tb01938.x.

Massman, J.M., Gordillo, A., Lorenzana, R.E., and Bernardo, R. (2013). Genomewide predictions from maize single-cross data. Theor. Appl. Genet. **126**:13–22. https://doi.org/10.1007/s00122-012-1955-y.

Masuda, Y. (1990). Auxin-induced cell elongation and cell wall changes. Bot. Mag. Tokyo **103**:345–370. https://doi.org/10.1007/BF02488646.

Miller, T.A., Muslin, E.H., and Dorweiler, J.E. (2008). A maize CONSTANS-like gene, conz1, exhibits distinct diurnal expression patterns in varied photoperiods. Planta **227**:1377–1388. https://doi.org/10.1007/s00425-008-0709-1.

Mu, Q., Guo, T., Li, X., and Yu, J. (2022). Phenotypic plasticity in plant height shaped by interaction between genetic loci and diurnal temperature range. New Phytol. **233**:1768–1779. https://doi.org/10.1111/nph.17904.

Munaro, E.M., Eyhérabide, G., D'Andrea, K.E., Cirilo, A.G., and Otegui, M.E. (2011). Heterosis×environment interaction in maize: what drives heterosis for grain yield? Field Crop. Res. **124**:441–449. https://doi.org/10.1016/j.fcr.2011.08.001.

Nicotra, A.B., Atkin, O.K., Bonser, S.P., Davidson, A.M., Finnegan, E.J., Mathesius, U., Poot, P., Purugganan, M.D., Richards, C.L., Valladares, F., and van Kleunen, M. (2010). Plant phenotypic plasticity in a changing climate. Trends Plant Sci. **15**:684–692. https://doi.org/10.1016/j.tplants.2010.09.008.

Ravi Kumar, S., Hammer, G.L., Broad, I., Harland, P., and McLean, G. (2009). Modelling environmental effects on phenology and canopy development of diverse sorghum genotypes. Field Crop. Res. **111**:157–165. https://doi.org/10.1016/j.fcr.2008.11.010.

Robertson, G.W. (1968). A biometeorological time scale for a cereal crop involving day and night temperatures and photoperiod. Int. J. Biometeorol. **12**:191–223. https://doi.org/10.1007/BF01553422.

Rojas, B.A., and Sprague, G.F. (1952). A comparison of variance components in corn yield trials: III. General and specific combining ability and their. Agron. J. **44**:462–466. https://doi.org/10.2134/agronj1952.00021962004400090002x.

Scheres, B., and van der Putten, W.H. (2017). The plant perceptron connects environment to development. Nature **543**:337–345. https://doi.org/10.1038/nature22010.

Shrestha, R., Gómez-Ariza, J., Brambilla, V., and Fornara, F. (2014). Molecular control of seasonal flowering in rice, arabidopsis and temperate cereals. Ann. Bot. **114**:1445–1458. https://doi.org/10.1093/aob/mcu032 %.

Shu, G., Cao, G., Li, N., Wang, A., Wei, F., Li, T., Yi, L., Xu, Y., and Wang, Y. (2021). Genetic variation and population structure in China summer maize germplasm. Sci. Rep. **11**:8012. https://doi.org/10.1038/s41598-021-84732-6.

Tamasloukht, B., Wong Quai Lam, M.S.-J., Martinez, Y., Tozo, K., Barbier, O., Jourda, C., Jauneau, A., Borderies, G., Balzergue, S., Renou, J.-P., et al. (2011). Characterization of a cinnamoyl-CoA reductase 1 (CCR1) mutant in maize: effects on lignification, fibre development, and global gene expression. J. Exp. Bot. **62**:3837–3848. https://doi.org/10.1093/jxb/err077.

Taylor, B.A., Cini, A., Wyatt, C.D.R., Reuter, M., and Sumner, S. (2021). The molecular basis of socially mediated phenotypic plasticity in a eusocial paper wasp. Nat. Commun. **12**:775. https://doi.org/10.1038/s41467-021-21095-6.

Via, S., and Lande, R. (1985). Genotype-environment interaction and the evolution of phenotypic plasticity. Evolution **39**:505–522.

Wang, Z., Pang, X., Lv, Y., Xu, F., Zhou, T., Li, X., Feng, S., Li, J., Li, Z., and Wu, R. (2013). A dynamic framework for quantifying the genetic architecture of phenotypic plasticity. Briefings Bioinf. **14**:82–95. https://doi.org/10.1093/bib/bbs009.

Whitman, D.W., and Agrawal, A.A. (2009). What is phenotypic plasticity and why is it important. In Phenotypic plasticity of insects: Mechanisms and consequences, pp. 1–63.

Wilczek, A.M., Roe, J.L., Knapp, M.C., Cooper, M.D., Lopez-Gallego, C., Martin, L.J., Muir, C.D., Sim, S., Walker, A., Anderson, J., et al. (2009). Effects of genetic perturbation on seasonal life history plasticity. Science (New York, N.Y.) **323**:930–934. https://doi.org/10.1126/science.1165826.

Xiao, Y., Jiang, S., Cheng, Q., Wang, X., Yan, J., Zhang, R., Qiao, F., Ma, C., Luo, J., Li, W., et al. (2021). The genetic mechanism of heterosis utilization in maize improvement. Genome Biol. **22**:148. https://doi.org/10.1186/s13059-021-02370-7.

Zeevaart, J.A.D. (2008). Leaf-produced floral signals. Curr. Opin. Plant Biol. **11**:541–547. https://doi.org/10.1016/j.pbi.2008.06.009.

Zhou, X., and Stephens, M. (2012). Genome-wide efficient mixed-model analysis for association studies. Nat. Genet. **44**:821–824. https://doi.org/10.1038/ng.2310.